Sensor Resonance and its Influence on the Measurement Results of Fast Transients

L. Kütt, M. Shafiq, M. Lehtonen, H. Mõlder, J. Järvik

***Abstract*-- Power line on-line condition monitoring can help improving the power supply reliability to great extent. One example of the effective condition monitoring methods is observing the intensity of the partial discharges. Accurate evaluation of partial discharge intensity is the key for a successful diagnostics, but this means also accurate recording of the whole transient that is initiated upon partial discharge (PD) occurrence.**

The partial discharge traces are pulsed transients with extremely short duration in their essence and bandwidth reaching into hundreds MHz is required for accurate acquisition. Rogowski coils and inductive loop sensors are one of the simplest current sensors that could be used for these purposes, as they provide bandwidth wide enough for this task. The accurate high frequency operation can still be rather difficult to achieve, as the sensor is set to operate close to the resonant conditions. Such resonance is present, for example, due to the inherent electrical properties dependent on geometrical dimensions of the sensor.

Within the paper, several scenarios are provided, where the inductive sensors are presented with different frequency response characteristics. It can be declared, that a resonance is the factor defining the upper frequency limit of a sensor bandwidth. An analysis is presented to show the effects of operation close to resonance frequency. Conclusions are drawn on the required characteristics of the sensor for measurement of partial discharge transients.

***Keywords*: Partial discharge, condition monitoring, pulsed transients, inductive current sensor, Rogowski current sensor, resonance.**

I. Introduction

A sensor is a device for sensing a physical quantity and providing output with a well-known relation to the sensed quantity. In electrical networks, sensors are used for providing a decoupled, low voltage reference of the high-voltage quantities (current and voltage) present on the high-voltage transmission systems. Most usual sensors in electrical substations are voltage and current transformers and measurement of electrical quantities in power networks is usually related to observing the 50 or 60 Hz sine quantities and their harmonic frequency components. The design of the voltage and current transformers has also focused on the 50 and 60 Hz measurements, at these frequencies the highest accuracy of the sensors is reached (usually from 5% up to 0,1%). The voltage and current harmonics have frequencies which are in multiples of the main frequency and in most application are observed up to 50th, which measurement frequencies up to 2500 or 3000 Hz respectively.

In terms of accuracy there are many characteristics that can provide an effect to it. One of the essential terms for electric sensors is the bandwidth. It is defined as frequency range from the lowest frequency up to the highest frequency, where the accuracy of the sensor is acceptable for the application. For different voltage and current transformers the operating bandwidth can be rather different. An example of this are well known issues related to harmonic measurements using the capacitive voltage transformers [1]. Measurements of pulsed phenomena are especially difficult tasks, as every pulse presents a very large variety of voltage and/or current components with different frequencies. Considering bandwidth of the sensor, the accurate capturing of a pulse requires a sensor to provide high accuracy for every frequency component. When the accuracy for the different frequency components is not guaranteed, the measurement of pulsed phenomena cannot be considered accurate.

This paper is focusing on the aspects of sensors with very wide measurement bandwidth. Uncommon to other measurements related to power systems, the sensors observed are low-power field sensors that are used for measurements in frequencies of MHz. For condition monitoring applications and especially for partial discharge measurements such sensors can provide several advantages.

There have been several papers published presenting the sensor characteristics and operation for partial discharge measurement [2], [3]. However, there is little actual comparison of the sensors properties and the sensor output for different frequency characteristics. This paper aims to complete the gap. In more practical considerations, content of this paper can be useful in selection of the sensors for the partial discharge monitoring as well as set-up and evaluation of their performance. For the utilities the accurate partial discharge on-line monitoring can provide a new level for insulation diagnostics.

Lauri Kütt, Muhammad Shafiq and Matti Lehtonen are with Aalto University Department of Electrical Engineering, 00076 Aalto, Finland (e-mail: lauri.kutt@aalto.fi; muhammad.shafiq@aalto.fi, matti.lehtonen@aalto.fi)

Heigo Mõlder and Jaan Järvik are with Tallinn University of Technology, Department of Electrical Engineering, 19086 Tallinn, Estonia (e-mail: heigo.molder@ttu.ee).

Paper submitted to the International Conference on Power Systems Transients (IPST2013) in Vancouver, Canada July 18-20, 2013.

II. Condition Monitoring using Partial Discharges

Measurement of short-duration transients has usually not been in the scope of interest for the power utilities. One reason for this is the essence of operation of the transmission grid, where the mains frequency sine-quantities are of primary importance. In more recent developments, attention to the means to observe the power line insulation condition has been growing. When insulation deterioration is minor but with some effect, extremely short (nano-micro second range) duration miniature breakdown events called partial discharges (PDs) occur in the problematic location. PD is the process of localized dielectric breakdown event in defects (cavities, voids, cracks or inclusions) of a solid or a liquid electrical insulation which is under high voltage stress [4]. As a result of each such PD occurrence, fast transient current pulse is generated due to sharp collapse of voltage across the defective cavity of insulation. This way, voltage and current transient is produced, presenting an electromagnetic wave which travels along the power line at speed of light. Measurement of these extremely fast pulses in substations can provide the information where the insulation degradation is happening, how far it has progressed and how fast it is progressing. If a potential defect is detected prior to complete breakdown it can help avoiding significant economic loss and customer dissatisfaction [5].

An example of a PD-pulse is presented below in Fig. 1, originating from a laboratory test set-up and PD-calibrator. Nevertheless, practical measurements have confirmed that it is rather identical to the actual average PD-waveform. The PD pulse has been measured using a high-frequency current transformer with 80 MHz bandwidth, which defines also the expected frequency content of the pulse. This PD-pulse will be used as a reference pulse in the following discussion.

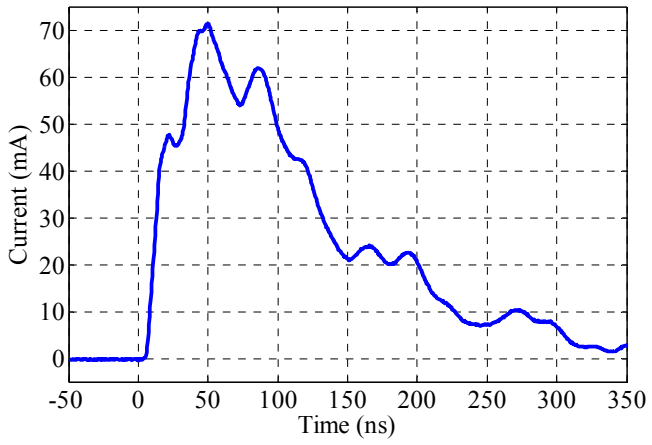

Fig. 1. Example of a partial discharge pulse.

III. Inductive Sensor Overview

For the accurate short-duration pulsed transient measurement, air-core inductive current sensors can be considered as a suitable option. The simple inductive loop (Fig. 2) as well as another type of this sensor, the Rogowski coil (Fig. 3), have been proposed for PD measurements also before [2], [3]. Its main benefit for the pulsed measurement applications is the wide operating bandwidth and sensitivity for the high-frequency range. In power systems this type of sensors have the benefits of fully uncoupled measurement capabilities, which is a virtue for measuring quantities associated with high-voltage power lines and equipment.

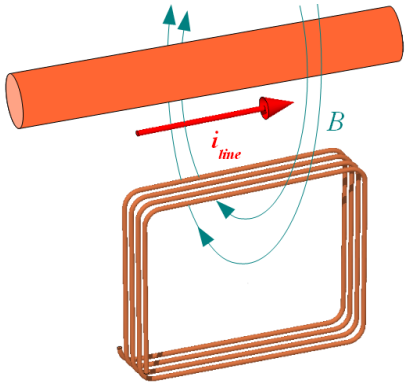

Fig. 2. Inductive current sensors overview. Simple inductive loop sensor.

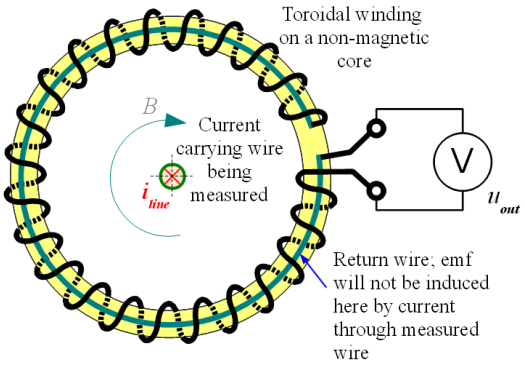

Fig. 3. Rogowski sensor is an array of loop sensors connected in series.

The inductive sensor is providing output reaction in response to magnetic field, result of the current passing through the wire. The output voltage u_{out} in simpler approach is a differential of the current variation rate

$$u_{out} = M_S \frac{di_{line}}{dt} \tag{1}$$

where M_S is the sensor mutual inductance, dependent on sensor geometry and number of turns [8]. For high-frequency operation, a more detailed model of the sensor needs to be considered, with clear role of the self-inductance and self-capacitance of the sensor. The circuit is described in Fig. 4 [6] as a RLC circuit for the medium-frequency range (10 kHz … 30 MHz), however for high frequencies and real cases this becomes even more complex. For the analysis of effects of sensor resonance, such model could still be considered sufficient, if the external circuits are considered as ideal.

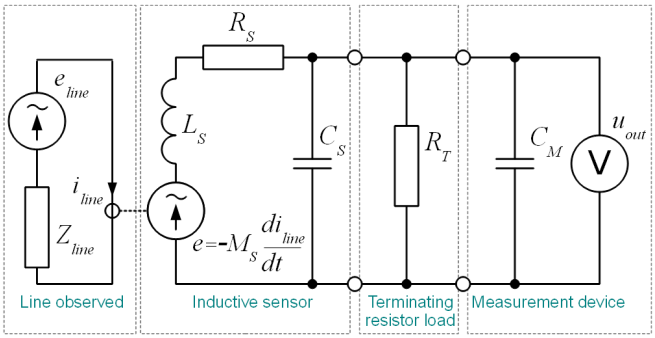

Fig. 4. Equivalent circuit of an inductive current sensor with measurement system connections.

In the equivalent circuit in Fig. 4, L_S, R_S and C_S represent the inductive sensor self-inductance, wire resistance and self-capacitance respectively. R_T is the termination or loading active resistor connected to the output terminals of the sensor and C_M is the measurement system input capacitance. In this context, the measurement probe resistance is assumed to be very high and is not represented as a separate component. R_S on the other hand is expected to be very small (< 1 Ω).

For more detailed sensor analysis in wide frequency range it is more appropriate to turn to the transfer function in *s*-domain. The transfer function can here be expressed as [9]

$$U_{out}(s)=\frac{s\cdot M_S\cdot I_{line}(s)}{L_S\cdot C_C\left[s^2+\left(\frac{1}{R_T\cdot C_C}+\frac{R_S}{L_S}\right)s+\left(\frac{1+\frac{R_S}{R_T}}{L_S\cdot C_C}\right)\right]} \quad (2)$$

where C_C is a sum of capacitances C and C_M connected in parallel.

Common to a RLC circuit, the transfer function is a second order function which can have oscillations in its transient response. There will be 2 poles for this transfer function, defining the resonance conditions. In addition, there is a zero which is due to differentiating nature of the sensor. Values of the poles provide information about the measurement set-up behavior and they can be found by solving the function of variable *s* found in the denominator.

Resonance of the second order circuit occurs when two poles provide a conjugate complex pair. In many practical set-ups this is true, provided the measurement device loading of the inductive sensor is light. A particular example of this is when oscilloscope probes that have, for example, 1 MΩ resistance, are used.

The inductive sensor is a good example of a sensor which can have oscillatory or non-oscillatory nature depending on some smaller changes introduced with the external components. In this paper, this sensor will be used to characterize the effects of resonance to the measurement results.

IV. Inductive Sensor Performance Scenarios

For the analysis of the sensor resonance, several scenarios are presented in the following. The inductive sensors with different high-frequency behavior are observed in the extremely short pulse measurements. The PD pulse presented above (see Fig. 1) will be used as an example of a transient for all scenarios. The magnitude and phase transfer plots are presented starting from frequency of 10 kHz, as the main content of the pulse is at relatively higher frequency values. All results have been scaled to provide theoretical transfer rate of 1.

A. Sensor with undamped oscillating transient response

Damping of the LC circuit can be achieved by having a lossy component (resistor) connected in the circuit. In the first example, a sensor having resonant frequency of 30 MHz is equipped with a high-impedance probe for measurement and $R_T=\infty$, which means that the output is practically undamped.

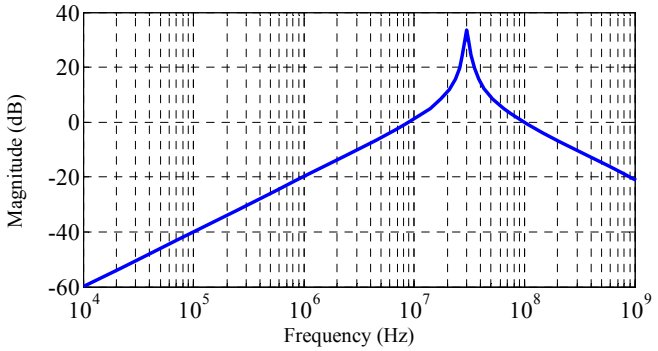

Fig. 5. Magnitude transfer plot for a sensor loaded with high-impedance probe, with resonant frequency of 30 MHz.

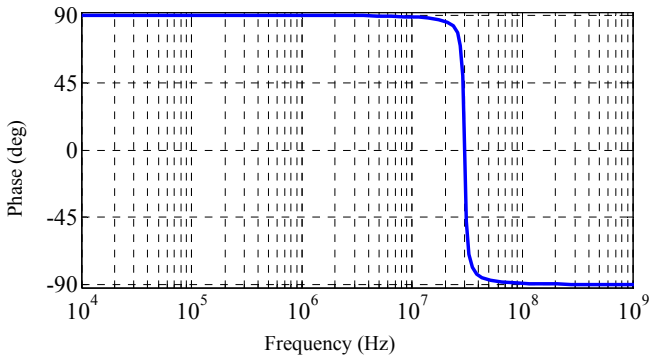

Fig. 6. Phase transfer plot for a sensor loaded with high-impedance probe, with resonant frequency of 30 MHz.

From the magnitude transfer plot of such a sensor (Fig. 5) the effect of differentiation is clearly visible, as with rising frequency the transfer rate is also becoming higher. Rate 20 dB/dec means that the amplitude transfer will increase 10 times when frequency is increased 10 times. The resonance point is clearly seen for frequency 30 MHz, where the magnitude transfer will see a sharper increase. For frequencies above the resonant the magnitude transfer will decrease with

rate of –20 dB/dec, presenting a filter for the higher frequency components.

Phase transfer plot (Fig. 6) presents phase shift of 90 degrees for the lower frequency range, provided as a result of the differentiation (see (1)). This will be turned by -180 degrees at the resonant frequency, effect caused by 2 poles in the same location, with every pole providing total of 90 degrees phase shift.

The simulation of the measurement (Fig. 7) of the sample pulse presents heavy oscillations in the sensor output, with the original nor the input differential waveform undetectable. The oscillations have very high portion compared to other information contained in the output which will present high noise for the measurement systems.

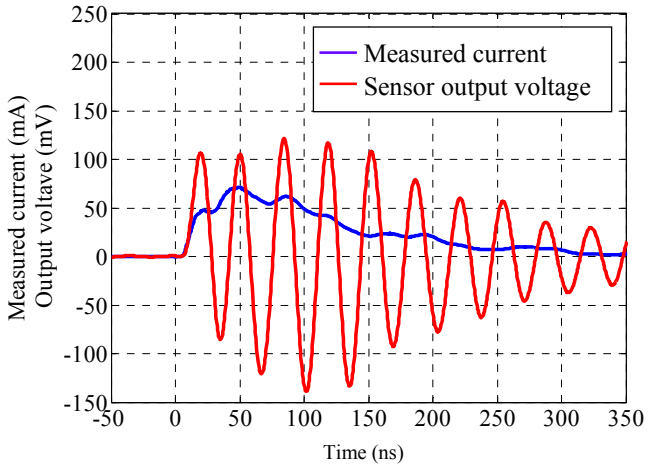

Fig 7. Output of sensor with 30 MHz undamped resonant response for a PD-pulse measurement.

In the applications where the signal from the sensor would be input to the analog to digital converter (ADC) for digital integration, such oscillations will require wide input voltage range. The true current differential in the output of the sensor will likely be closer the noise level in this case.

B. Undamped sensor operation with ideal integrator

For obtaining the original current waveform from the differentiated output (1), the output of the sensor would need processing with an integrating unit. A low-pass filter RC circuit, which is also known for its integrating properties, could be used for this. Ideal integrator adds a pole at frequency zero in the sensor system transfer function (2). The case example for this is observing similar model with 30 MHz resonant frequency, presented also in case A.

It should be pointed out from the magnitude transfer plot resulting from adding an integrator (Fig. 8) that the filtering effect after the 30 MHz range is quite strong, presenting a -40 dB/dec decrease for the frequencies above 30 MHz. For 100 MHz frequency component this means over 6 times decrease in transfer rate. The integration provides change to phase transfer characteristic as well, when for low frequencies the phase shift is decreased from 90 degrees to 0 degrees (Fig. 9), which is actually beneficial for pulse measurement.

The integrated output signal presents also clear resonant oscillations with high intensity. At this time, there is no use of filtering the 30 MHz oscillations, as then much of the useful signal is also lost.

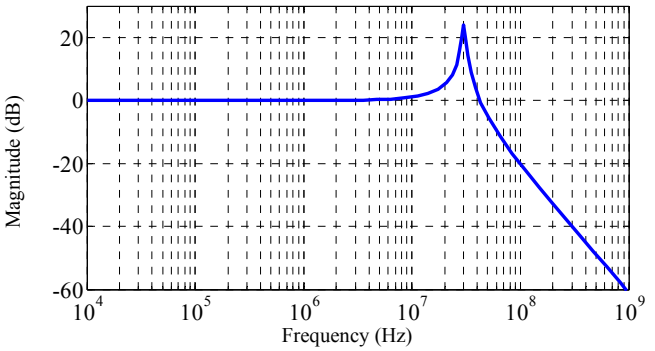

Fig. 8. Magnitude transfer plot for a sensor with resonant frequency of 30 MHz after ideal integration of the output signal.

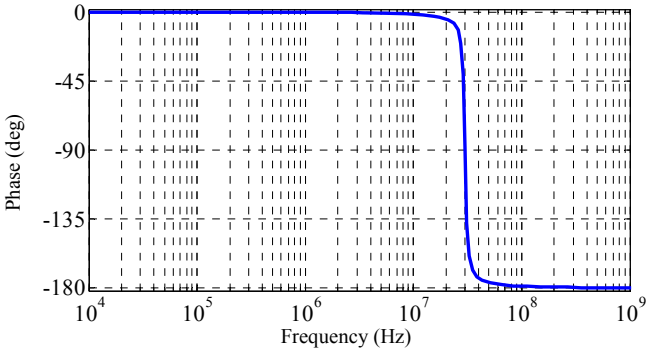

Fig. 9. Phase transfer plot for a sensor with resonant frequency of 30 MHz after ideal integration of the output signal.

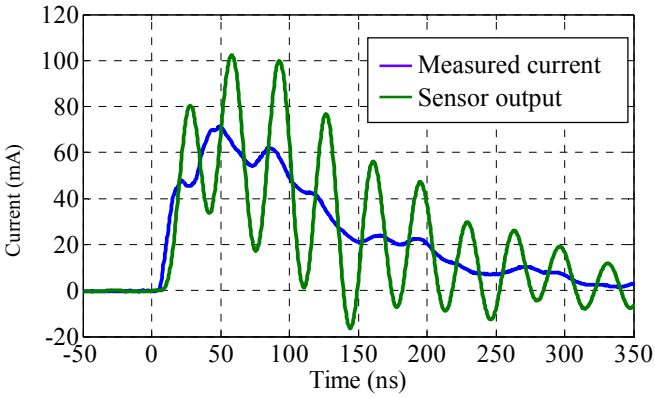

Fig. 9. Measurement result of a sensor with resonant frequency of 30 MHz after ideal integration of the output signal.

In case of real integration circuits and also digital integration (or summing) a lower bandwidth limit, where the integration effect is starting from is usually defined. An example of scenario where the integration lower bandwidth is starting from 100 kHz has been presented in Fig. 10. The oscillations are again clearly observable in the output result in Fig. 11, however some comparison of the output is made later in the discussion section.

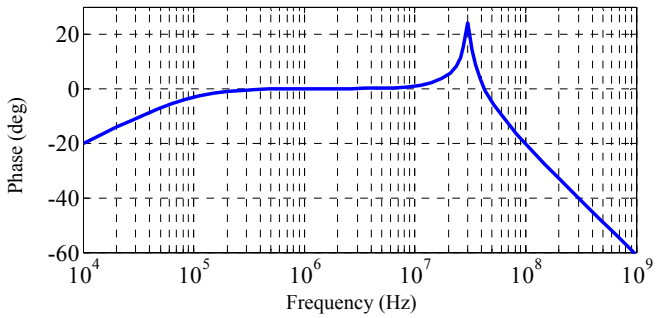

Fig. 10. Magnitude transfer plot for a sensor with resonant frequency of 30 MHz after integration of the output signal starting from 100 kHz.

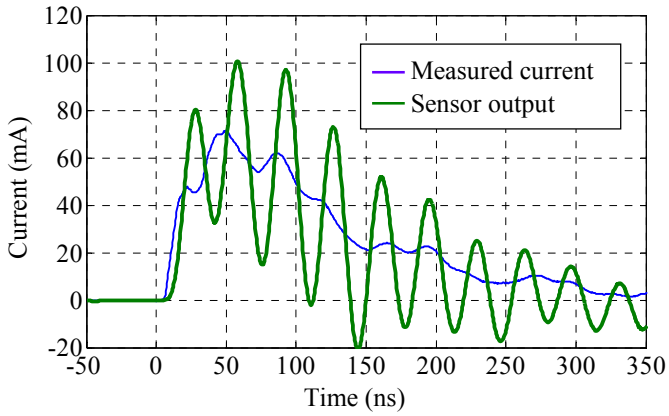

Fig. 11. Measurement result of a sensor with resonant frequency of 30 MHz after integration of the output signal.

C. Undamped sensor with high resonant frequency

A question arising is how high the resonant frequency should be, so that it would not provide significant set-back in the accuracy. For comparison a scenario can be presented, revealing the sensor system operation provided the resonant frequency was at 5 times higher frequency than observed previously (i.e 150 MHz). The results of the simulations for this case are presented in Fig. 12.

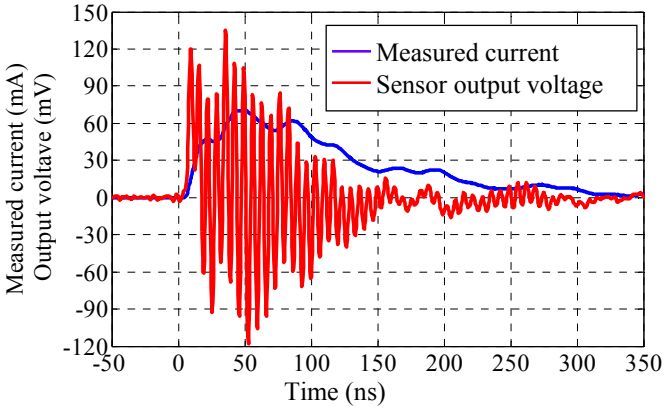

Fig 12. Output of sensor with 150 MHz undamped resonant response for a PD-pulse measurement.

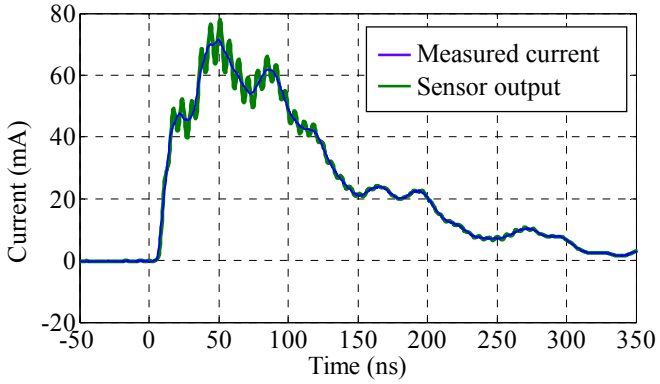

Fig. 13. Measurement result of a sensor with resonant frequency of 150 MHz after ideal integration of the output signal

The measured current pulse contains highly many different frequency components and the circuit is still excited enough to cause clearly visible oscillations in the output of the sensor. The frequency content of the pulse is however mostly below 150 MHz and because of this the resonance is not initiated with magnitude as significant as for the previous scenario, where the resonant frequency of the sensor was at 30 MHz. In present case a filter working at the resonant frequency could be used, however it has to be kept in mind, that the filter has some effect on lower frequency ranges also.

When adding an ideal integrator to the sensor with 150 MHz resonant frequency (Fig. 13), a near-perfect match is revealed. In this case some reservations have to be stated, as the sample pulse acquisition bandwidth has been 80 MHz. This means that the components close to the sensor resonant frequency have lower magnitude values, and effects introduced by the sensor resonance would be comparatively small. As the PDs are weaker, their duration is also shorter and then also higher frequencies provide more significant effect, which again can lead to similar oscillations as discussed with Fig. 9.

Here also a case where the integrator lower bandwidth is introduced could be observed for comparison. This will cause deviation from the input as the pulse duration increases.

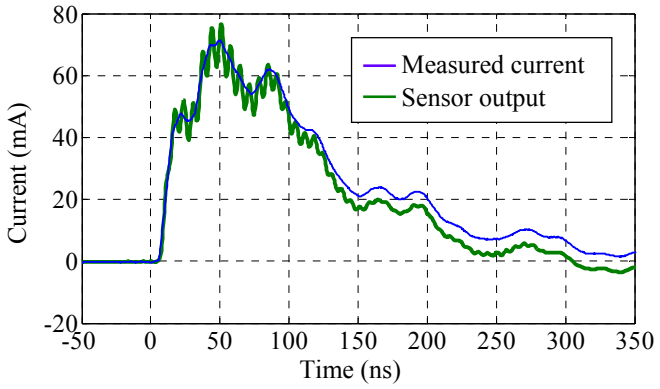

Fig. 14. Measurement result of a sensor with resonant frequency of 150 MHz after integration of the output signal.

V. NON-RESONANT OPTIONS

Damping of the resonant oscillations can be achieved using a suitable lossy resistor R_T connected to the output of the sensor. When the load of the circuit is increased the resonance has smaller and decaying effect, until the critical damping is reached [7]. In this case the sensitivity of the sensor is intact for frequency below the resonance, however the oscillations are not present in the output. This way a true differential of the input current can be reached, provided the sensor bandwidth (i.e resonance) is at high enough frequency. A comparison of the critically damped sensor outputs and the respective integration results are provided in Fig. 14 and Fig. 15. In practical aspects it has to be kept in mind that building a sensor with 150 MHz resonant frequency and acceptable sensitivity could be rather challenging.

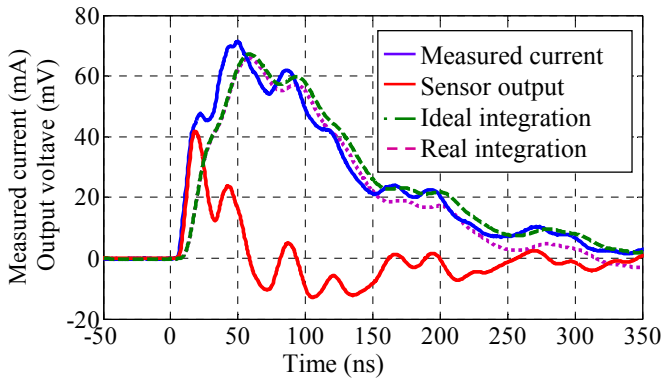

Fig. 14. Comparison of measurements with a critically damped sensor with resonant frequency of 30 MHz.

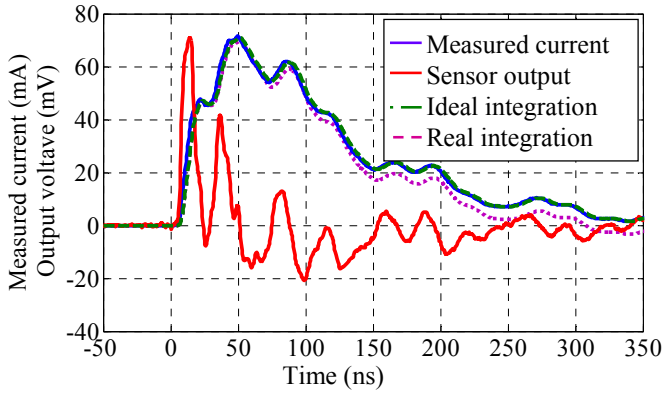

Fig. 15. Comparison of measurements with a critically damped sensor with resonant frequency of 150 MHz.

Loading the circuit with resistive components even more will lead to an overdamped state. The sensitivity of the sensor starts decreasing as resistance value of the load is decreased. As the PD signals have very low energy, it could be a problem if detection of even smallest PD traces is required. Nevertheless, overdamping can also provide measurement functionality, unreachable with the output integration and damping of the resonance. Namely, in the overdamped region the 2 poles that were at the same frequency for the resonant cases now have different frequencies. One of the poles has relatively small frequency while the other pole has relatively high frequency. While the load resistance decreases, the poles shift further away from each other. With this, a "self-integrating" region is created, as the lower frequency pole is actually performing the same task as in previous examples was handled by the added integrator part.

The example is presented with 2 poles, one at 0.1 MHz and the other at 150 MHz. This actually can be achieved using a sensor with undamped mode resonant frequency of 30 MHz. For the self-integrating region the magnitude transfer as well as the phase transfer plots present high stability at 0 dB and 0 degrees respectively. Compared to examples above, the suitable stable operational bandwidth for pulse measurement reaches well beyond the identified undamped mode resonance point. It can be declared that the low frequencies are not critical as the measured pulses do not present significant content in the very low frequency areas.

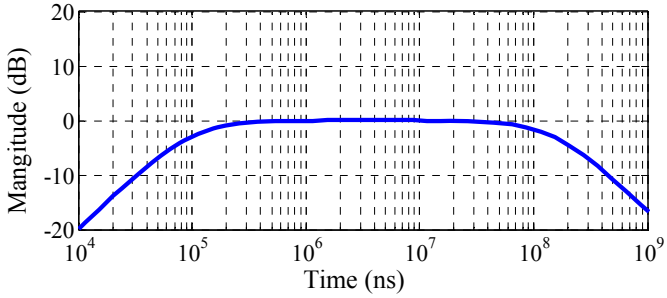

Fig. 16. Magnitude transfer plot for a sensor with resonant frequency of 30 MHz after integration of the output signal starting from 100 kHz.

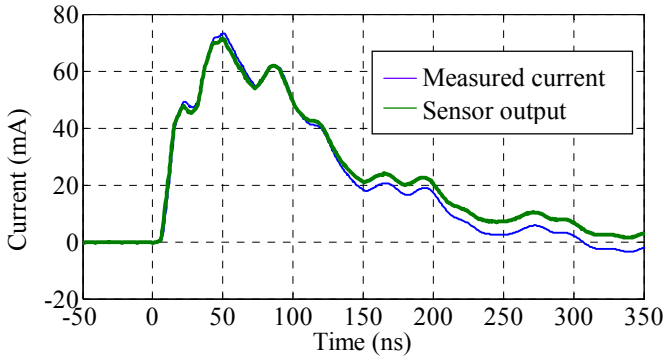

Fig. 17. Magnitude transfer plot for a sensor with resonant frequency of 30 MHz after integration of the output signal starting from 100 kHz.

The plot in Fig. 17 presents a quite nice match between measured signal and the output. Error visible in the end of the transient can be traced to not having sufficient low-frequency sensitivity. This is valid for all the sensors observed with limited integrating bandwidth.

Configuration without resonance is more recommended still, as the lack of resonance at any frequency will mean that there would be any oscillations caused by the sensor itself. This will provide least noise in the output of the sensor.

VI. Results and discussion

PDs are quantified using terms of charge. For the PD evaluation, the partial discharge magnitude can be obtained by observing the integration result of the current passing through the wire during the transient. This can be used also for comparison of the output results of different scenarios.

TABLE I
COMPARISON OF PD MEASUREMENT RESULTS USING DIFFERENT SENSOR CONFIGURATIONS, COMPARED TO REFERENCE RESULT OF 22.9 NC.

Sensor configuration	PD charge evaluation result, nC	Difference from reference, %
Resonant at 30 MHz, ideal integration	25.4	10.9
Resonant at 30 MHz, limited integration	24.1	5.2
Resonant at 150 MHz, ideal integration	23.0	0.4
Resonant at 150 MHz, limited integration	20.1	12.2
Damped at 30 MHz, ideal integration	22.9	0.0
Damped at 30 MHz, limited integration	20.0	12.7
Damped at 150 MHz, limited integration	20.1	12.2
Overdamped with poles at 0.1 and 150 MHz	20.2	11.8

Comparison of the results reveals that the sensor with resonant operation at 30 MHz would provide quite significant error by itself. The limited integration cases when the integration lower bandwidth was limited, the error is also quite significant, however this is caused more due to the lack of sensitivity in the lower frequency regions. The bandwidth limit in higher frequency ranges will on the other hand cause distortions to the measured pulse acquired waveform, as seen from Fig. 14.

Observed examples provided the cases, when the resonance is originated from the sensor itself. There are many other possible components and aspects also for the measurement systems that can provide resonance, like the measurement system wires, measurement system input etc [9]. Presence of resonance would provide significant noise and it would need to be guaranteed that there was as little resonance as possible involved with the measurement set-ups. Resonance is one effect to be avoided in the measurement systems.

After the resonant frequency has been reached the filtering effect becomes very intense (see Fig. 8), also the phase transfer plot presents significant phase shift (Fig. 9). It can be declared that the resonant frequency is the highest frequency that the sensor could be used reliably to observe. Components with higher frequency than resonance will likely be significantly damped. For measurement of pulses this can provide significant error in the results.

VII. Conclusions

Inductive air-core sensors can be highly beneficial for the measurement of high-frequency transients and extremely short pulses, partial discharge being one of such. These sensors on the other hand can be subjected to self-resonance, which can provide significant oscillations in the output signal, which is noise for the measurement system and can cause significant errors in the measurements.

Out of several cases presented in this paper, the case with added load in the output of the sensor can be named as preferable. Reaching the overdamped operation, the sensor self-resonance is no longer a problem. Also, with the correct configuration, the output quality can be reached that was previously available with additional external integrator. Downside of the additional loading of the sensor output will be the decreased sensitivity.

For the sensor set-ups for field measurements, the air-core sensors are advised to be tested first for resonance, as the real environment holds much electromagnetic noise. Self-resonance due to noise can provide false peaks and false alarms, making the measurement unreliable.

VIII. References

Periodicals:

[1] Yao Xiao, Jun Fu, Bin Hu, Xiaoping Li, Chunnian Deng, "Problems of voltage transducer in harmonic measurement", IEEE Transactions on Power Delivery, Vol. 19, No. 3, Jul 2004, pp. 1483 – 1487.

[2] G. M. Hashmi, M. Lehtonen, M. Nordman, “Modeling and experimental verification of online PD detection in MV covered-conductor overhead networks,” IEEE Trans. Dielectr. Electr. Insul., Vol. 17, No. 1, Feb 2010, pp. 169–180.

[3] M. Argüeso, G. Robles, J. Sanz, “Implementation of a Rogowski coil for the measurement of partial discharges”, Rev. Sci. Instrum. 76, 065107 (2005).

[4] P. Valatka, V. Sučila, G. Daukšys, "Investigation of the Voltage Influence on Partial Discharge haracteristic Parameters in Solid Insulation", Electronics and Electrical Engineering, No.10 (106), 2010, pp. 63–66.

[5] G.J. Paoletti, A. Golubev, "Partial discharge theory and technologies related to medium-voltage electrical equipment", IEEE Transactions on Industry Applications, Vol. 37, Jan/Feb 2001, pp. 90 – 103.

[6] M. Shafiq, L. Kütt, M. Lehtonen, T. Nieminen, G. M. Hashmi, “Parameters Identification and Modeling of High Frequency Current Transducer for Partial Discharge Measurements”, IEEE Sensors Journal, Vol. 13, Iss. 3, Mar 2013, pp. 1081 - 1091.

[7] M. Shafiq, L. Kütt, M. Isa, M. Hashmi, M. Lehtonen, “Directional Calibration of Rogowski Coil for Localization of Partial Discharges in Smart Distribution Networks”, International Review of Electrical Engineering, Vol. 7, No. 5, 2012, pp. 5881-5890,

Papers from Conference Proceedings (Published):

[8] M. Rezaee,, H. Heydari, Mutual inductances comparison in Rogowski coil with circular and rectangular cross-sections and its improvement; 3rd IEEE Conference on Industrial Electronics and Applications, 2008 (ICIEA 2008); pp. 1507 – 1511.

[9] L. Kütt, J. Järvik, H. Mõlder, J. Kilter, S. Muhammad, Magnetic Current Sensor Stray Components in High Frequency Operation and their Effects, 11th Conference on Environment and Electrical Engineering (EEEIC) 2012, 6 p.